JOURNAL OF MATERIALS SCIENCE 13 (1978) 113–118

X-ray diffraction studies of $GdFe_2$ Mössbauer samples

D. C. CREAGH
Physics Department, Royal Military College, Duntroon, A.C.T. 2600, Australia
S. H. AYLING
139 Signals Squadron, Enoggera, Queensland 4052, Australia

X-ray diffraction techniques have been used to determine the lattice parameters and stacking fault probabilities of specimens of the cubic Laves phase compound $GdFe_2$ used in Mössbauer experiments. The lattice parameter for most samples was 7.400 ± 0.005 Å. All the samples exhibited high stacking fault probabilities. The stacking fault probabilities lay in the range 0.12 to 0.35.

1. Introduction

The cubic Laves phase compound $GdFe_2$ has been extensively studied recently using Mössbauer techniques because the nature of the hyperfine field can give useful information on the Gd–Fe and Fe–Fe exchange interactions. The initial experiments on $GdFe_2$ were conducted by Bowden *et al.* [1]. The spectrum at 77 K contained six spaced lines, but because of the asymmetry in line intensities and line profiles they concluded that the easy direction of magnetization was *not* aligned along a principal symmetry axis. Later work by Atzmony and Dariel [2] yielded a symmetrical six-line Mössbauer spectrum, and, with the use of a curve-fitting procedure they were able to conclude that the easy directions of magnetization were aligned along the ⟨1 0 0⟩ directions. They ascribed the failure of Bowden's experiment to poor specimen preparation. In a later experiment van der Velden *et al.* [3] found Mössbauer spectra very similar to those found by Bowden *et al.* Subsequently Cashion [4], and Price [5], have investigated the Mössbauer spectrum of $GdFe_2$. Their spectra were also similar to those reported by Bowden *et al.*

The spectrum obtained using the Mössbauer technique indicates whether or not the iron atoms lie in equivalent positions with respect to the direction of magnetization. If some of the iron atoms lie in inequivalent positions with respect to the direction of magnetization both the amplitudes and positions of the lines in the Mössbauer spectrum are changed. With the exception of the spectra observed by Atzmony and Dariel [2] all the spectra show that inequivalent iron sites are present, and the question must be asked: is the reason for this connected, as Atzmony and Dariel assert, with faulty specimen preparation techniques? This paper describes X-ray diffraction studies of the samples used by Bowden *et al.*, Cashion and Price.

In preparing for the X-ray study, a literature search was conducted to establish what the lattice parameter a_0 is for the $GdFe_2$. Nine values were quoted [6–13] ranging from 7.355 to 7.53 Å. Specimens measured by Savitskii *et al.* [7, 13] had values 7.36 and 7.53 Å respectively. Most of the measurements, however, lay in the range 7.39 ± 0.01 Å. Since the relative error in the lattice parameter quoted by most authors was 0.04% it is evident that either they were optimistic about the accuracy of their experiments or the lattice parameter of $GdFe_2$ depends on the thermal history and composition of the $GdFe_2$. In this paper we shall discuss some of the difficulties encountered in the measurement of the lattice parameter for $GdFe_2$.

2. Experimental techniques

2.1. Sample preparation

Table I summarizes the techniques by which the various samples of $GdFe_2$ were manufactured. The

TABLE I Summary of the details of specimen manufacture and analysis

Reference	Manufacture*	Final state	Annealing	X-ray analysis†
[1]	aa, s	powder	argon	diff
[2]	aa, ex	powder	vacuum, 1200 K 1 week	DS
[3]	aa, s and ex	powder	vacuum, 1300 K 2 weeks	DS
[4]	aa, s	powder	–	diff
[5]	eb, s and ex	powder	vacuum, 1100 K 2 weeks	diff
		bulk	unannealed	diff
[5]	aa, s	powder	unannealed	diff
		bulk	unannealed	diff

*aa = argon arc, eb = electron beam, s = stoichiometric, ex = excess of gadolinium.
†diff = diffractometer, DS = Debye–Scherrer camera.

samples which were not made at the Royal Military College were all prepared in argon arc furnaces. An intimate mixture of gadolinium powder and iron powder was prepared and then melted in an arc struck in a chamber containing pure argon gas. When the desired temperature (1350 K) was reached the molten mixutre was quenched rapidly to room temperature. The solid button was turned over and the process repeated. This remelting procedure was performed several times to ensure homogeneity of composition within the specimen. For the samples manufactured at the Royal Military College an electron beam furnace was used. The mixture of gadolinium and iron powders was pressed firmly in an extrusion press using a 10 mm diameter indium die. The compacted mixture was then placed on the hearth of a Planar Electron Beam Furnace. When the chamber had been evacuated to a pressure of 10^{-6} Torr the electron beam was focused onto the surface of the mixture and the mixture became molten. After the electron beam was interrupted the ingot solidified quickly because the hearth of the furnace was water cooled. The specimen was removed, turned over and the sequence repeated several times to ensure homogeneity of composition within the specimen.

Bowden *et al.* [1], Cashion [4], and Price [5] used samples which had been manufactured using the exact stoichiometric ratio of gadolinium to iron. Van der Velden [3] and Price [5] used a number of samples which were mixed either in exact stoichiometric proportions or with 2 to 5 wt% more gadolinium than one would have in a stoichiometric mixture. Atzmony and Dariel [2] always used between 5 and 15 wt% more gadolinium than would be required for a stoichiometric mixture. This, they said, compensated for the higher vapour pressure of the rare-earth component and ensured that the solidified ingot was rich in the rare-earth component.

After manufacture the buttons were crushed, ground, or filed in an inert atmosphere. The resulting powder was then wrapped in tantalum foil and annealed at high temperatures in a high vacuum. The annealing process was usually continued for a week or more.

The annealed powders were then examined using X-ray diffraction techniques. Atzmony and Dariel [2] used a Debye–Scherrer camera and determined the lattice parameter using the NRTS extrapolation technique [14, 15]. A similar procedure was used by van der Velden *et al.* [3]. The samples analyzed by Bowden *et al.* [1], Cashion [4] and Price [5] were examined using X-ray diffractometers.

2.2. X-ray techniques

2.2.1. X-ray equipment

To ensure the widest possible data base for the X-ray analysis of Mössbauer samples two completely different X-ray systems were used. One, a Rigaku SG-7 horizontal diffractometer, was mounted on a Rigaku D9C generator in which was mounted a chromium fine-focus X-ray tube. A standard Rigaku electronics panel was used for the collection of the pulses generated in the Xenon proportional detector which was mounted on the detector arm of the diffractometer. The second system consisted of a vertically mounted Rigaku 2122B3 diffractometer which was connected to a mains stabilized Philips PW 1120 generator. A molybdenum fine-focus X-ray tube generated the X-rays which were detected by a Xenon proportional detector and analysed by a high stability

Ortec nucleonic system. For one series of experiments an incident beam crystal monochromator was used, but because there appeared to be no significant advantage in its use the majority of the results reported here were made using conventional techniques.

Because the positions of the peaks of the Bragg reflections must be known accurately the diffractometers were calibrated each day using both a silicon powder specimen and an annealed bulk aluminium specimen. Both continuous rotation ($\frac{1}{4}^\circ$ 2θ per minute) and step scan recordings were made. Scans were made in both the clockwise and anticlockwise direction. The continuous rotation data was used for the measurement of the lattice parameter and the step scan data was used for the analysis of the low order ($h^2 + k^2 + l^2 < 20$) reflections.

The Bowden and Cashion samples were provided as pressed powder pellets. For both the electron beam melted and argon arc-melted specimens used by Price a more comprehensive set of specimens was created. The ingots of $GdFe_2$ were first mounted in a Servomet spark erosion machine and cut into two or more parts. The surfaces were then etched with nital until about 100 μm had been removed from the surface. This was sufficient to render the surfaces free of the damage caused in the process of spark machining. After X-ray analysis, one of the surfaces was rendered into a powder form by crushing or filing under alcohol. The powder was then pressed lightly with a collodion binder to form a specimen for X-ray and Mössbauer analysis. One would expect that the effect of the cold work would have had a significant influence on both the position and shape of the X-ray lines. (See, for example, Warren [16].) This was not the case. There was only a small shift in the position of the lines and some minor increase in their integral breadths. Some specimens were later annealed at 1100 K for periods of a week or more.

2.2.2. Measurement of the lattice parameter a_0

In this paper the $\cos\theta \cot\theta$ extrapolation procedure suggested by Adler and Wagner [17] has been used to eliminate the effect of systematic errors associated with the diffractometers and their alignment. For chromium radiation the maximum value of $(h^2 + k^2 + l^2)$ which can be observed is 32. For molybdenum radiation the maximum value of $(h^2 + k^2 + l^2)$ used in the determination of a_0 was 100. In Figure 1 the value of $a(h, k, l)$ derived from the measurement of the Bragg angle θ of the $h\,k\,l$ reflection is plotted as a function of $\cos\theta \cot\theta$. This figure is typical of the data acquired during this study; the upper graph is for molybdenum radiation and the lower graph for chromium radiation. Note the scatter of the points about the lines of best fit. The points marked with their $h\,k\,l$ values are of particular significance. For all the X-ray data, as with the graphs shown here, the points corresponding to 1 1 1, 2 2 0, 4 0 0 and 4 2 0 reflections lie below the line whilst the 2 0 0, 3 1 1 and 2 2 2 points lie above the line. Their displacements from the line are much greater than one would expect from random errors in the measurement of Bragg angles. This pattern of peak shifts suggests a crystallographic rather than a random origin for the displacements of the peaks. The values of the lattice parameter for the specimens investigated in this paper are set out in Table II.

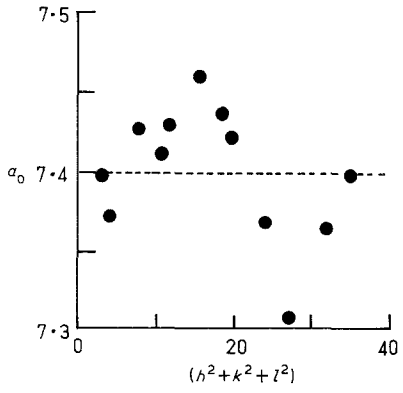

Figure 1 The value of the lattice parameter calculated from the Bragg angle θ of the $h\,k\,l$ reflection is plotted as a function of $\cos\theta \cot\theta$ for (a) Mo$K\alpha_1$ and (b) Cr$K\alpha_1$ radiation. Each of the low order reflections is identified by its Miller indices.

2.2.3. The peak shift

The space lattice of the $GdFe_2$ lattice is f c c. Warren [16] has summarized the effect of faulting

TABLE II Lattice parameters a_0 and stacking fault probabilities α for the various sets of Mössbauer samples

Reference	a_0 (Å)	α
[5]	7.400 ± 0.005	0.23 ± 0.11
[5]	7.401 ± 0.005	0.35 ± 0.27
[1]	7.380 ± 0.005	0.32 ± 0.20
[4]	7.408 ± 0.009	0.12 ± 0.06

in f c c structures. It is assumed that the source of faulting is due to changes in the sequence of close packed {1 1 1} planes. The translation vectors of the conventional lattice $\mathbf{a}_i$ can be changed to translation vectors of a hexagonal lattice $\mathbf{A}_i$ by the transformation

$$\begin{aligned} \mathbf{A}_1 &= -\mathbf{a}_1/2 + \mathbf{a}_2/2 + 0 \\ \mathbf{A}_2 &= 0 \quad -\mathbf{a}_2/2 + \mathbf{a}_3/2 \\ \mathbf{A}_3 &= \mathbf{a}_1 \quad +\mathbf{a}_1 \quad +\mathbf{a}_3 \end{aligned} \tag{1}$$

The Miller indices of the hkl plane in the conventional structure now become

$$\begin{aligned} H_0 &= -h/2 + k/2 \\ K_0 &= \quad -k/2 + l/2 \\ L_0 &= h \quad +k \quad +l. \end{aligned} \tag{2}$$

The scattering power of the lattice can then be written in terms of the new hexagonal axes. In normal stacking, the {1 1 1} planes are stacked in the sequence ABCABCAB .... If, however, a deformation fault exists, one plane or part thereof is missing. The stacking sequence is then ABCBCAB .... The probability of finding a deformation fault is denoted as α and $1/\alpha$ is a measure of the number of layers between faults. For growth (or twin) faults the stacking sequence is ABCBAC. The probability of a growth fault occurring is denoted as β. Warren [16] has shown that deformation faults give rise to a shift in the position of the peak of a line and also can cause line broadening. Growth faults cause asymmetrical line broadening. After the Rachinger correction [18] for the presence of $K\alpha_2$ radiation has been applied the line profiles are symmetrical. Thus it is reasonable to assume that deformation rather than growth faults are present in the specimens.

The shift in the peak of a reflection is then given by:

$$\Delta(2\theta) = \frac{90\sqrt{(3)}\tan\theta}{\pi^2 h_0^2(\mathrm{u}+\mathrm{b})}\,\alpha \sum_{\mathrm{b}} (\pm) L_0. \tag{3}$$

Here the line shift is $\Delta(2\theta)$ degrees; θ is the Bragg angle for a reflection of type hkl; L_0 equals $h+k+l$; h_0^2 equals $h^2+k^2+l^2$; and u + b is the total number of combinations of hkl for the reflection. Of these the components corresponding to $L_0 = 3M$ give rise to unbroadened lines, (u). Those corresponding to $L_0 = 3M \pm 1$ are broadened and the summation of L_0 is taken only for these broadened components, (b). Warren has tabulated the value of

$$\frac{1}{h_0^2(\mathrm{u}+\mathrm{b})} \sum_{\mathrm{b}} (\pm) L_0, \tag{4}$$

for a number of low index reflections. Positive values of this summation correspond to shifts in the peak of the line to higher values of Bragg angle, and hence lower apparent lattice parameter. Negative values correspond to shifts to lower values of Bragg angle and hence larger apparent lattice parameters. Table III sets out the values of the summation for those reflections for which $h_0^2 < 20$. Included on this table is an indication of the direction of the experimental peak shift. In every case the direction of the peak shift is the same as that predicted by theory.

TABLE III Comparison of the measured direction of peak shift with the theoretical direction of peak shift

hkl	$\sum_{\mathrm{b}} \frac{(\pm) L_0}{h_0^2(\mathrm{u}+\mathrm{b})}$	Expt. shift
1 1 1	$+\frac{1}{4}$	+
2 0 0	$-\frac{1}{2}$	−
2 2 0	$+\frac{1}{4}$	+
3 1 1	$-\frac{1}{11}$	−
2 2 2	$-\frac{1}{8}$	−
4 0 0	$+\frac{1}{4}$	+
3 3 1	$+\frac{10}{57}$	+
4 2 0	$-\frac{1}{20}$	−

In their initial experiment Warren and Warekois [19] compared the line shift in an unannealed specimen with that for an annealed specimen. Such a procedure is not possible in the case of $GdFe_2$ because annealing does not appear to have much effect on either the line positions or their widths. Evidently the faulting is frozen in when the molten specimen is quenched. One must therefore know the value of the lattice parameter to a high degree of accuracy. Having assessed the value of the lattice parameter one can then calculate the position of the Bragg reflection and estimate the line shift by subtracting from the calculated Bragg angle the experimentally determined Bragg angle. For each specimen the values of $\Delta(2\theta)$ for the 1 1 1, 2 0 0, 2 2 0, 3 1 1, 2 2 2, 4 0 0 and 4 2 0 were found using this procedure, and in every case the direction of the line shift was predicted by theory. Using Equation 3 the stacking fault parameter α can be calculated. The values shown in Table II show a large experimental error. This does not

mean that each set of measurements on a particular specimen possessed a large statistical error. For example, for the specimen from which the data shown in Fig. 1 was derived the value of α was found to be 0.22 ± 0.02. The variation between the values of α for different specimens may be due to variations in the stacking fault probability within an ingot but is more likely to be dependent upon the state of the surface under investigation. Such was the case for both the Bowden and Cashion samples. Removal of material from the surface of these powder specimens did affect the value of α in a random manner.

3. Discussion

For the $GdFe_2$ made using the electron beam furnace the analysis of fifteen bulk and twelve powder samples yielded a lattice parameter of 7.400 ± 0.005 Å. For the argon arc melted samples [5] ten separate samples in both bulk and powder form had lattice parameters of 7.401 ± 0.005 Å. Both of the sets of specimens had a well known thermal history and had been subjected to X-ray analysis at all stages of preparation. Of the other specimens the Cashion specimen had a slightly larger lattice parameter, 7.408 ± 0.009 Å, whilst the Bowden specimen had a much lower lattice parameter 7.380 ± 0.005 Å. The thermal histories of these two samples are not well documented and it is therefore difficult to suggest a reason why these two specimens should differ from the previous specimens. The results of all the experiments suggest that neither the method of melting the powders together nor minor variations in composition of the mixture has a significant effect on the lattice parameter. It may be that the factors such as the rate of quenching are of significance. The effects of quenching and annealing on cubic Laves phase compounds are currently being investigated at R.M.C. using a high temperature furnace mounted on the Rigaku 2122B3 diffractometer. No conclusive evidence as to the effects of quenching and annealing is yet to hand.

Klug and Alexander [20] have listed the parameters which may cause errors in the measurement of lattice parameters. Of these only the zero-angle calibration is a constant. This has been eliminated by careful alignment procedures and by frequent checks against both a silicon powder and a bulk aluminium specimen. All the other parameters (e.g. specimen displacement, specimen transparency, type of soller slits, the use of a flat

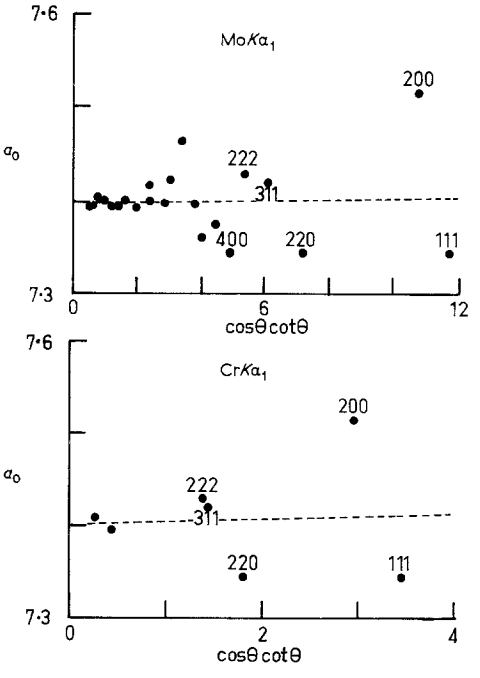

Figure 2 The effect of systematically rejecting data on the extrapolated value of a_0 is demonstrated. The ordinate is the value of $h^2 + k^2 + l^2$ at which the extrapolation commences.

specimen) give rise to peak shifts of lower values of 2θ, the shift being proportional to $\cos\theta$ and $\cot\theta$. The peak shifts observed in this study cannot be explained in terms of the mis-setting of, and defects of, the instrumentation. One might argue, however, that the position of each observed peak is influenced by the instrumental parameters and that the $\cos\theta\ \cot\theta$ extrapolation procedure is still a valid one. That this is not necessarily the case is demonstrated in Fig. 2. In this figure the apparent value of the lattice parameter derived from the application of the $\cos\theta\ \cot\theta$ extrapolation to the data of Fig. 1 as a function of the omission of data points from the analysis. The lattice parameter was first found by using the extrapolation to fit all the 25 indexed reflections. Then it was found for the case when the 1 1 1 reflection was omitted; then with the 1 1 1 and 2 0 0 reflections omitted; and so on. The apparent value of a_0 oscillates markedly about the value 7.400 Å. Clearly extrapolation procedures ought not to be applied unless one knows the positions of all the reflections and has some knowledge of the state of deformation of the specimen. The foregoing remarks are valid for all similar extrapolation procedures, e.g. the NRTS

extrapolation [14, 15] often used for the resolution of data recorded by Debye–Scherrer cameras.

The $GdFe_2$ lattice (Structurbericht C15) is a f c c lattice containing eight molecules per unit cube. The stacking faults lie in {1 1 1} planes and are bounded by Shockley partial dislocations of the ⟨2 1 1⟩ type. The density of stacking faults observed in the course of these experiments is high: on average every fourth of fifth {1 1 1} plane contains a stacking fault. Assuming that the average dimension of a stacking fault is approximately four times the {1 1 1} interplanar spacing one can estimate the stacking fault energy using Ayling's [21] data for the yield strength of $GdFe_2$. The estimated stacking fault energy of 20 ergs cm^{-1} is comparable with values found for a wide range of metals and alloys.

The Mössbauer results of all workers except Atzmony and Dariel show the lack of a unique hyperfine field. A distribution of hyperfine fields is possible in the faulted $GdFe_2$ specimens since the iron atoms which provide the major part of the hyperfine field lie in sheets parallel to the {1 1 1} planes, and in the region of a fault the distance between the layers of iron atoms is not the same at it would be for an undeformed lattice. Because the iron atoms are tetrahedrally co-ordinated with one another the variation in the close packing of the planes due to the stacking fault also causes local variations in the directions of the hyperfine field. This also affects the Mössbauer spectrum. The fact that Atzmony and Dariel have recorded spectra which show a unique hyperfine field can thus be taken as an indication that their samples contained a low stacking fault density.

Acknowledgements

The authors are grateful to Dr F. Bowden, Dr J. Cashion, and Mr A. Vass for the provision of $GdFe_2$ specimens, and to Dr D. Price for his analysis of the specimens using the Mössbauer facility at the Australian National University.

References

1. G. J. BOWDEN, D. St. P. BUNBURY, A. P. GUIMARES and R. E. SNYDER, *J. Phys. C.* **2** (1968) 1367.
2. U. ATZMONY and M. P. DARIEL, *Phys. Rev. B.* **10** (1974) 2060.
3. J. N. J. VAN DER VELDEN, A. M. VAN DER KRAAN, P. C. M. GUBBENS and K. H. J. BUSCHOW, Conferences Digest No. 3, Rare Earths and Actinides, Durham, (1971) p. 191.
4. J. CASHION, private communication (1976).
5. D. PRICE, to be published (1977).
6. M. MANSINAM and W. E. WALLACE, *J. Chem. Phys.* **40** (1964) 1167.
7. E. M. SAVITSKII, V. F. TEREKHOVA, I. V. BUROV and O. D. CRYSTYAKOV, *Zh. Neorgan Khim* **6** (1961) 1732.
8. N. C. BAEZIGER and J. L. MORIARTY, *Acta Cryst.* **14** (1961) 948.
9. J. H. WERNICK and S. GELLER, *Trans. AIME* **218** (1960) 866.
10. K. NASSAU, L. V. CHERRY and W. E. WALLACE, *J. Phys. Chem. Solids* **16** (1960) 123.
11. W. M. HUBBARD and E. ADAMS, *J. Phys. Soc. (Japan)* **17** (1962) 143.
12. E. A. SKRABEK, Ph.D. Thesis, Pittsburg (1962).
13. E. M. SAVITSKII, V. F. TEREKOVA and I. V. BUROV, *Zh. Neorgan Khim* **7** (1962) 169.
14. J. B. NELSON and D. P. RILEY, *Proc. Phys. Soc. (London)* **57** (1945) 160.
15. A. TAYLOR and H. SINCLAIR, *ibid* **57** (1945) 126.
16. B. E. WARREN, "X-ray Diffraction" (Addison–Wesley, Massachusetts, 1969).
17. R. P. I. ADLER and C. N. J. WAGNER, *J. Appl. Phys.* **33** (1962) 3451.
18. W. A. RACHINGER, *J. Sci. Instru.* **25** (1948) 254.
19. B. E. WARREN and E. P. WAREKOIS, *J. Appl. Phys.* **24** (1953) 951.
20. H. P. KLUG and L. E. ALEXANDER, "X-ray Diffraction Procedures" (John Wiley and Sons, New York, 1974).
21. S. H. AYLING, B.Sc. Honours Thesis, University of New South Wales, (1975).

Received 31 March and accepted 28 April 1977.